# Section 7


# Global and regional climate models, sensitivity and impact experiments, response to external forcing

# Changes in wetland methane emissions in the IAP RAS global model under RCP anthropogenic scenarios

S. N. Denisov, M.G. Akperov, M. M. Arzhanov, A.V. Eliseev, V.S. Kazantsev, N.V. Pankratova,
M.A. Dembitskaya, Yu. A. Shtabkin, E.V. Berezina

A.M. Obukhov Institute of Atmospheric Physics, RAS, Moscow, Russia

*denisov@ifaran.ru*

The sensitivity of methane emissions in the Northern Hemisphere to the North Atlantic Oscillation (NAO) variability was estimated for the second half of the 20th century. To simulate methane fluxes from natural wetlands, we used a methane emissions scheme (Denisov et al. 2010, 2013). Model estimations of methane fluxes and their variations were made using the time series of monthly data CRU TS3.1 for the near-surface temperature, precipitation and cloud cover in 1960-2009. Other characteristics were taken from the full version of the A.M. Obukhov Institute of Atmospheric Physics RAS global climate model (IAP RAS GCM). For analysis we selected 5 years with the highest NAO index (1 for each decade in 1960-2009 period) and correspondingly 5 years with the lowest NAO index for winter (DJF). The comparison of methane fluxes was performed for the upcoming warm period.
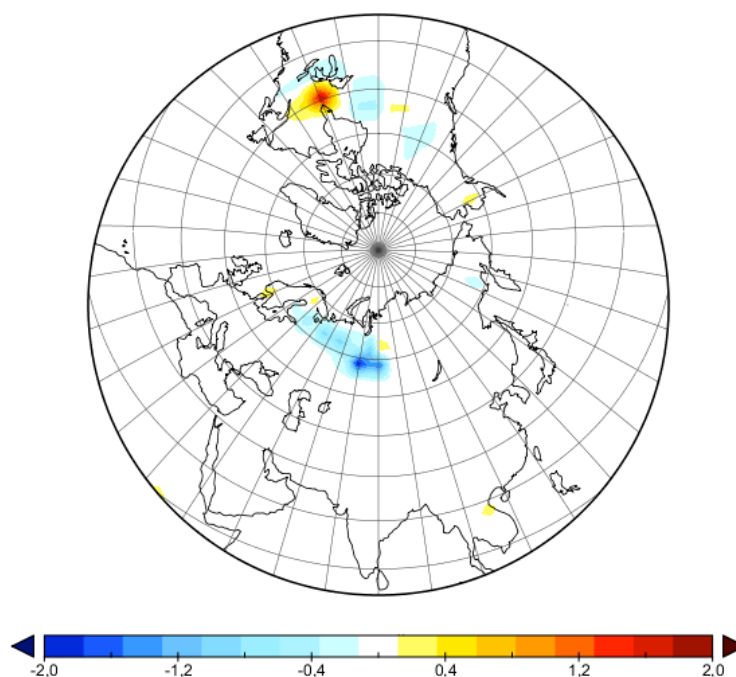


Figure 1. The difference in methane emission [$gCH_4/m^2/year$] between years with the highest and the lowest NAO indices.

The estimated methane emissions from the western Siberian wetlands are approximately 2 gCH4/m2/year higher in the positive phase of NAO than in its negative phase (Fig.1). The difference is about 20% of the average methane emission for the second half of the 20th century. A strong interannual variability of methane emissions was noted for this region so such a difference can be partly explained without taking into account its connection with NAO. But it should be noted that methane emissions strongly depend on the near-surface atmospheric temperature and rainfall during the cold season.

The linkage of these characteristics with abnormal values of the NAO index to some extent determines the anomalous character of methane emissions in the following years.

**References**

Denisov S.N., Eliseev A.V., Mokhov I.I. Assessment of changes in methane emissions from marsh ecosystems of northern eurasia in the 21st century using regional climate model results. *Russian Meteorology and Hydrology.,* 2010, 35(2), 115-120.

Denisov S. N., Arzhanov M.M., Eliseev A. V., Mokhov I. I. Climate change in IAP RAS global model taking account of interaction with methane cycle under anthropogenic scenarios of RCP family. *Russian Meteorology and Hydrology.,* 2013, 38(11), 741-749.

# Climate change and extreme precipitation: the response by a convection-resolving model

Michel Déqué, Antoinette Alias, Samuel Somot and Olivier Nuissier
Centre National de Recherches Météorologiques (CNRS/CNRM), Météo-France.
42 avenue Coriolis F-31057 Toulouse Cédex 1, France, michel.deque@meteo.fr

Among expectations from global warming, caused by anthropic greenhouse gases emissions, many studies have pointed out the increase in precipitation above a certain threshold, also known as extreme precipitation increase. This feature is common to most climate models, including those with a very coarse resolution. It is not incompatible with a decrease in total precipitation, i.e. the accumulation for all precipitating days. It is also in agreement with Clausius-Clapeyron law, which states that temperature is a limiting factor for atmosphere moisture. However IPCC global models represent poorly the probability distribution function of precipitation beyond 99% percentile. Therefore a model consensus is not enough to definitely state that extreme precipitations will increase during the 21st century. Regional climate models, in particular those running at 12 km horizontal resolution like in EuroCordex, attempt to represent phenomena closer than the observed ones. However both GCMs and RCMs do not explicitly represent the physical phenomenon responsible for heavy rainfall, i.e. convection.

The climate of the South-East part of France, named Mediterranean climate, is characterized by heavy rainfall in autumn and early winter. It is still debatable whether these phenomena have increased or not during the 20th century. In this region, the eastern part of the Massif Central mountain (so-called Cevennes) undergoes the maximum daily rainfall rates with observed values above 300 mm/day in the SOND season, based on the last decade records. Almost every year, dramatic flash flood events are reported there, and the link to climate change is often pointed out.

In order to explore the role of an explicit representation of the convection in the simulation of heavy precipitation, two experiments have been carried out. In each experiment we have used ALADIN (Déqué and Somot, 2008), a hydrostatic model with 12 km resolution on a domain covering France and surrounding areas, and AROME (Seity et al., 2011) a non-hydrostatic model with 2.5 km resolution on a smaller domain centered on South-East France. ALADIN provides lateral boundary conditions to AROME. Both models are operational forecast models at Météo-France, and may be used for long climate simulations as well (e.g. in Cordex).

The first experiment is a validation against the hourly 1kmx1km 1997-2006 rainfall reanalysis over France COMEPHORE (Tabary et al., 2012) based on radar and rain gauges. ALADIN is driven by the ERA-interim reanalyses, and drives in turn AROME. We have selected 0.5°x0.5° boxes where the maximum daily rainfall exceeds 300 mm in the daily 8kmx8km reanalysis over France SAFRAN (1989-2014). This domain corresponds broadly to the above-mentioned Cevennes region. For COMEPHORE, AROME and ALADIN, all the grid points of this domain for SOND 1997-2006 are aggregated, and a cumulative distribution function (cdf) is calculated. This operation is done for hourly as well as for daily rainfall. Figure 1 shows the tail of the cdfs (in fact 1-cdf). The probability estimated is the absolute probability, not a conditional one. Thus, a probability of 0.00001 for hourly data corresponds to a return period of 35 years at a given grid point. For daily data, this probability corresponds to 24 times this length. The ALADIN daily cdf is poorly sampled at the very tail, with 1220 days and 124 grid points in the "Cevennes" domain. For AROME (3097 grid points) and COMEPHORE (22500 gridpoints) the sampling used to evaluate a 0.00001 probability is better. One can see that the high resolution model AROME is closer to observations than ALADIN, even though AROME underestimates rainfall for probabilities less than 0.001.

It is not surprising that a model at lower resolution produces less extreme events than a model with higher resolution. The interesting question is: do the two models behave similarly in a global warming scenario. If yes, one can use Cordex model responses as a proxy, with a statistical adjustment (e.g. quantile mapping) when realistic amounts are needed in an impact study. If no, we need to run regional models at the highest possible resolution, when the impact study is connected with extreme precipitation. The second experiment consists in two pairs of simulations with ALADIN and AROME. The driving condition is an RCP8.5 scenario with CNRM-CM5 model (CMIP5 experiment). The first time slice, named reference, is 1989-2000. The second, named scenario, is 2089-2100.
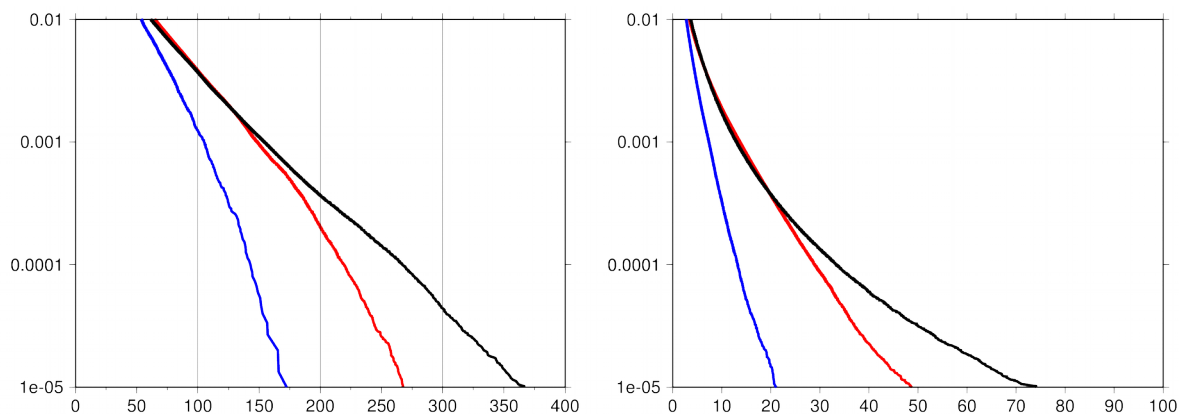
**Figure 1**: Tail of the complement to one of the cumulative distribution function for daily (left) and hourly (right) precipitation (mm) in the Cevennes area for the validation experiment: COMEPHORE (black), AROME (red) and ALADIN (blue); probabilities are shown in logarithmic scale.

Figure 2 shows the tail of the cdfs for hourly and daily precipitation, AROME and ALADIN, reference and scenario. For hourly precipitation (right panel), the expected behavior is obtained: both models increase the extreme precipitation. For daily precipitation (left panel), an opposite behavior is observed: AROME decreases the extremes whereas ALADIN increases them, in agreement with the usual behavior of GCMs and RCMs.
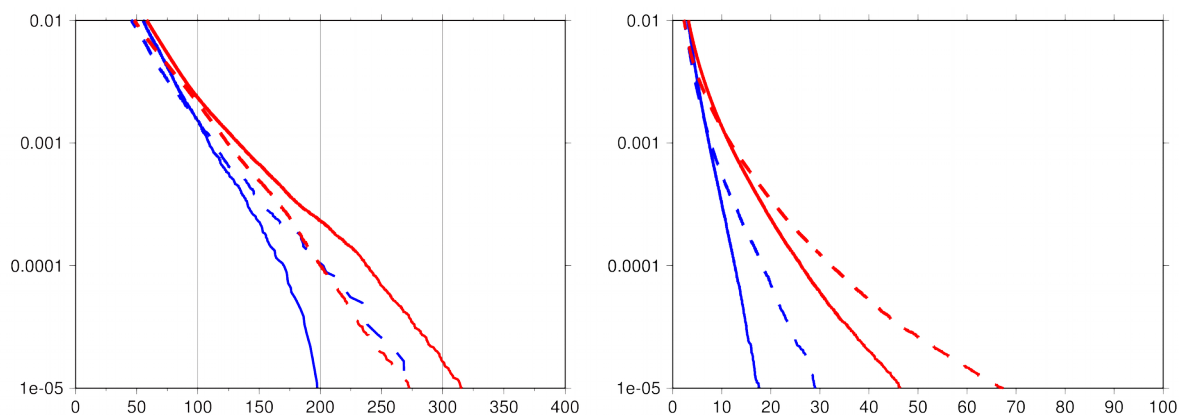


**Figure 2**: As Figure 1 for AROME (red) and ALADIN (blue); reference time slice (solid line) and scenario time slice (dash line).

We should avoid to generalize this result: the analysis period is only 12 years, and on other parts of the domain both models increase the extreme daily precipitations. But we want to report here that one must be careful when using GCMs or hydrostatic RCMs to evaluate the response of climate change on extreme precipitation events.

**References:**

Déqué, M., and Somot, S. 2008. Added value of high resolution for ALADIN Regional Climate Model. Idöjaras Quaterly Journal of the Hungarian Meteorological Service, 112(3-4), 179-190.

Seity, Y., Brousseau, P., Malardel, S., Hello, G., Bénard, P., Bouttier, F., Lac, C., and Masson, V., 2011. The AROME-France convective scale operational model, Monthly Weather Review, 139, 976-991.

Tabary, P., Dupuy, P., L'henaff, G., Gueguen, C., Moulin, L., Laurantin, O., Merlier, C., and Soubeyroux, J.M., 2012. A 10-year (1997–2006) reanalysis of Quantitative Precipitation Estimation over France: methodology and first results. Weather Radar and Hydrology, IAHS Publ. 351, 255-260.

# Changes of atmospheric blockings in the 21st century from CMIP5 ensemble simulations with RCP scenarios

Mokhov I.I., Timazhev A.V.

A.M. Obukhov Institute of Atmospheric Physics RAS
mokhov@ifaran.ru

The largest regional climate anomalies are related to atmospheric blocking anticyclones (blockings). Significant consequences associated with changes in the blocking activity can be expected under global warming [1] (see also [2, 3, 4]). We analyze here possible changes of atmospheric blockings from the CMIP5 ensemble simulations with different RCP scenarios in the 21$^{st}$ century.

There are significant differences in characteristics of blockings detected by various methods. Here we compare blocking characteristics detected by the methods described in [6] (LO), [7] (PH) and [5] (BEA). Different versions of BEA-method were used with different restrictions for the blocking (with radius $R$) shift pR for 1-day step. In particular, we used here p = 0.3, 0.4, 0.5.
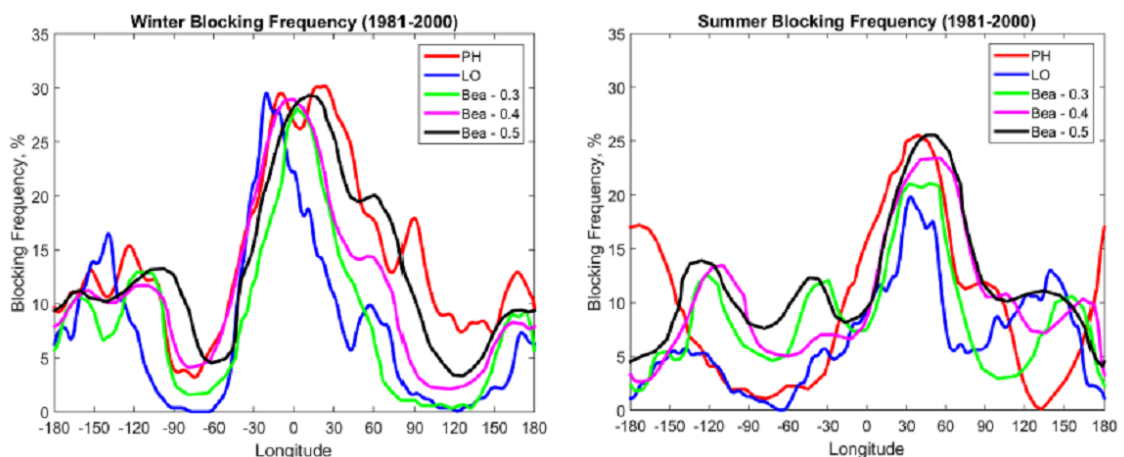


Fig. 1.

Figure 1 shows characteristics of winter and summer blocking frequency detected by several methods from NCEP/NCAR reanalysis data (1981-2000) for different longitudes in the Northern Hemisphere: PH, LO and BEA (3 versions with p = 0.3, 0.4, 0.5).

Possible changes of atmospheric blockings were estimated from the CMIP5 ensemble simulations with 10 model versions, in particular, BCC-CSM1, BCC-CSM1 - M, GFDL-CM3, GFDL-ESM2G, HadGEM2-ES, IPSL-CM5A-LR, IPSL-CM5A-MR, MIROC-ESM-CHEM, MRI-CGCM3, NorESM1-M.

Figure 2 presents changes of blocking frequency in summer and winter for the Euro-Atlantic region (60W-60E) between 2071-2100 and 1976-2005 from the total ensemble model simulations with the RCP 4.5 scenario. Similar changes are presented in Fig. 2 for selected ("best") models. The ensembles of "best" models were selected from the condition of maximum correlation of longitudinal distributions of seasonal-mean blocking frequency from model simulations and NCEP/NCAR reanalysis data for the period 1976-2005.
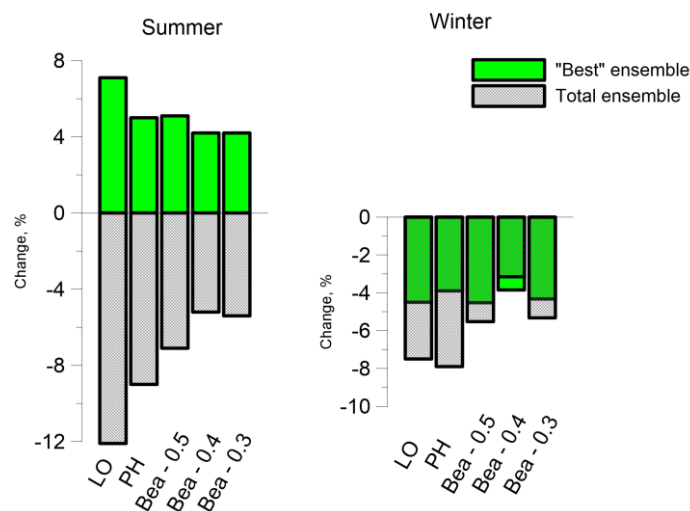
Fig. 2.

According to Fig. 2 the uncertainty of estimates for the blocking frequency is larger for summer than for winter. Such estimates were obtained for different regions in the Northern Hemisphere and for various RCP scenario. This work was supported by the RFBR and RAS. Different methods for the atmospheric blockings detection were compared in the framework of the RSF project (14-17-00806).

**References**
1. IPCC, 2013: Climate Change 2013: The Physical Science Basis. Contribution of Working Group I to the Fifth Assessment Report of the Intergovernmental Panel on Climate Change. [T.F. Stocker, D. Qin, G.-K. Plattner et al. (eds.)]. Cambridge Univ. Press, Cambridge, 1535 pp.
2. Mokhov I.I., M.G. Akperov, M.A. Prokofyeva, A.V. Timazhev, A.R. Lupo and H. Le Treut, 2013: Blockings in the Northern Hemisphere and Euro-Atlantic region: estimates of changes from reanalysis data and model simulations. *Doklady Earth Sci.*, **449**(2), 430–433.
3. Mokhov I.I., A.V. Timazhev and A.R. Lupo, 2014: Changes in atmospheric blocking characteristics within Euro-Atlantic region and Northern Hemisphere as a whole in the 21st century from model simulations using RCP anthropogenic scenarios. *Glob. Planet. Change*, **122**, 265-270.
4. Mokhov I.I. and A.V. Timazhev, 2015: Model assessment of possible changes of atmospheric blockings in the Northern Hemisphere under RCP scenarios of anthropogenic forcings. *Doklady Earth Sci.,* **460**(1), 63-67.
5. Bardin M., G.V. Gruza, A.R. Lupo, I.I. Mokhov and V.A. Tikhonov, 2005: Quasistationary anticyclones in the Northern Hemisphere: An analysis of interannual and interdecadal variability and long-term trends at 1000 hPa and 500 hPa using a geometric definition. *Proc. 16th Symp. on Global Change and Climate Variation, 85th Ann. Meet. AMO*, 9-13.
6. Lejenas H. and H. Okland, 1983: Characteristics of Northern Hemisphere blocking as determined from a long time series of observational data, *Tellus A,* **35**, 350–362.
7. Pelly J.L. and B.J. Hoskins, 2003: A new perspective on blocking. *J. Atmos. Sci.,* **60**, 743–755.

# Spatiotemporal structure of changes in carbon dioxide and oxygen fluxes through the surface of Arctic seas in changing climate

Nadyozhina E.D., I.M.Shkolnik, A.V.Sternzat, R.S.Bortkovskii
Voeikov Main Geophysical Observatory, 7, Karbyshev str., 194021, St.Petersburg, Russia

The balance of $CO_2$ and $O_2$ in the Arctic seas is maintained by a complex of interplaying processes. Rapidly evolving changes in the balance of these gases can lead to deterioration of marine ecosystems, their irreversible modification or collapse. Numerous studies have shown that the Arctic seas (AS) provide a sink of $CO_2$ that amounts from 25% to 50% of its anthropogenic emissions into the global atmosphere (Totterdell, 2013; Borges et al., 2006; Sabine et al., 2004). Thus, the AS substantially contribute to mitigation of greenhouse effect. The role of AS can change in the future if water temperature continues to increase along with sea ice retreat. This will result in changing the intensity of gas exchange between the atmosphere and sea. Many studies have discussed possible impacts of alternate changes in $CO_2$ fluxes, driven by global climate evolution in XXI century, on regional ecosystems. Shift in carbon balance due to global warming may lead to AS acidification, which in turn can cause negative implications for marine biota.

The question over how the ongoing climate change in XXI century will affect gas fluxes in the polar regions, and what are the accompanying uncertainties, is essential. The primary goal in the gas exchange analysis is connected with clearer understanding of flux-related physical processes in the atmosphere and the ocean. Here the analysis of "atmosphere-ocean" gas exchange over the Arctic seas using gas exchange model (Bortkovsky, 2006) driven by CMIP5 and MGO pan-Arctic RCM climate change simulations is conducted (Shkolnik and Efimov, 2013). The gas exchange model model accounts for gas transfer by bubbles under strong wind conditions by including source (sink) members in the gas exchange equations. Provided that global (regional) climate models generate an input for the model, it can calculate intensity of $CO_2$ and $O_2$ fluxes.

Here the spatiotemporal patterns of $CO_2$ and $O_2$ fluxes through the surface of the Barents, Kara, Laptev and East-Siberian seas are analysed. Each of the seas is characterized by specific features: shelf structure, currents, salinity, depth, amount of fresh water input from rivers. The study aims at analysis of changes in $CO_2$ and $O_2$ fluxes over AS under projected evolution of global and regional climate system.

## References

Borges A.V., Schiettecatte L.S., Abril G., Delille B., Gazeau E., 2006. Carbon dioxide in European coastal waters. Estuarine Coastal Shelf Sci. 70 (3), 375–387.

Bortkovskii R.S., 2006. On the estimate of the mean exchange with $CO_2$ and $O_2$ between atmosphere and ocean in the key regions of the World's ocean. Izv RAS, Fizika atmospheri i okeana, Vol. 42, 2, pp. 250-257.

Sabine C.L. et al., 2004. The oceanic sink for anthropogenic $CO_2$. Science 305, 367–371.

Shkolnik I.M. and S. V. Efimov, 2013. Cyclonic activity in high latitudes as simulated by a regional atmospheric climate model: added value and uncertainties *Environ. Res. Lett.* 8 045007.

Totterdell I. Impacts of climate change on air-sea exchanges of $CO_2$ Marine Climate Change Impacts Partnership: Science Review MCCIP 2013: 91-97 doi:10.14465/2013.arc11.091-097.

# Dangerous hydrological events in future climate as projected by an ensemble of high resolution RCM for northern Eurasia

Igor Shkolnik, Tatiana Pavlova and Sergey Efimov
Voeikov Main Geophysical Observatory, 7, Karbyshev str., 194021, St. Petersburg, Russia

The evidence of modeling projections of climate change impacts on floodings is important for water resources management and flood assessment by decision-makers. Impact models usually use climate projections provided by global and regional climate models (RCM). However, challenges in representing dangerous hydrological events over the river catchments suggest that decisions should be made depending on the degree of realism of runoff simulation by an RCM at high resolution. Given an RCM simulated surface and groundwater inflow to rivers, the river routing model can compute flow and volume of water everywhere across watersheds taking into consideration the multitude of feeders.

Here to simulate future changes in flood frequency and intensity over the northern Eurasia the CaMa-Flood river routing model (Yamazaki et al., 2011) is used. The model is driven by runoff derived from an ensemble of ten decadal long RRCM (Shkolnik and Efimov, 2015) simulations spanning 1990-1999 and 2050-2059 ($10\times2=20$ simulations in total). The horizontal grid size of RRCM is $381\times183$ with a mesh width of 25 km. All the simulations differ in the atmospheric initial and time dependent lateral boundary conditions, provided by an AGCM T42L25. The experiments include SST/IC evolution as projected by three most successful CMIP5 models using IPCC RCP8.5 scenario.

Given that modeling runoff, being a small difference of the two large values (precipitation and evaporation), is prone to significant biases due to biases in water balance components, it needs to be calibrated (corrected for bias) to be used for an input in the CaMa-Flood model. The quality of the simulated river discharge is evaluated through comparison of RCM-driven river routing model output with river discharge observations at 43 level gauges across watersheds of northern Eurasia. Simulated changes in the mean and extreme water discharge over the river network in northern Eurasia at resolution $0.25°\times0.25°$ are considered. Possible changes in flood area (Fig.1), flood depths and flood water volume are analyzed in the context of projection uncertainties.
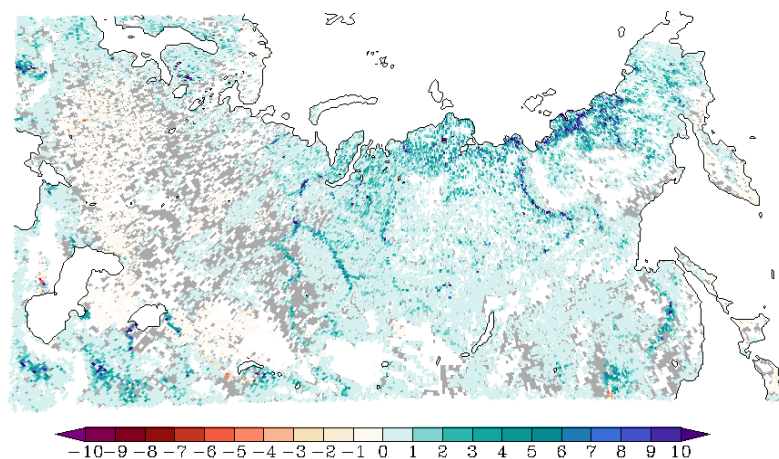
Fig. 1 Changes (%) in the annual maximum flood area by 2050-2059 relative to 1990-1999 as simulated by 10-member ensemble of RRCM at 25 km resolution under IPCC RCP8.5 scenario.

**References**

Shkolnik I.M., Efimov S.V. (2015), A new generation regional climate model for northern Eurasia. Proceedings of MGO, Vol. 576, pp. 201—211.

Yamazaki, D., S. Kanae, H. Kim, and T. Oki (2011), A physically based description of floodplain inundation dynamics in a global river routing model, Water Resour. Res., 47, W04501, doi:10.1029/2010WR009726.

# The schedule of the Mul'tanovskii's synoptic periods

Nikolay S. Sidorenkov

Hydrometeorological Research Center of the Russian Federation, Moscow

sidorenkov@mecom.ru

This contribution is a continuation of the paper (Sidorenkov, Zhigailo, 2014).

The lunar-solar tides deform the Earth's shape and change the Earth's moment of inertia. As a result, they have a noticeable effect on the velocity of the Earth's daily rotation. The tidal oscillations of the Earth's rotation rate over any time interval can be calculated theoretically (Sidorenkov, 2002, 2009). By way of illustration, Figure 1 shows the tidal deviations of the Earth's daily angular velocity $v$ in 2016. The Earth's rotation velocity is characterized by the relative value (Sidorenkov, 2002, 2009)

$$v \equiv \frac{\delta\omega}{\Omega} = \frac{\omega - \Omega}{\Omega} \approx -\frac{\Pi_E - T}{T} \equiv -\frac{\delta\Pi}{T},$$

where $\Pi_E$ is the length of Earth's day; $T$ is the length of the standard (atomic) day, which is equal to 86400 s; and $\omega = \frac{2\pi}{\Pi_E}$ and $\Omega = \frac{2\pi}{86400}$ rad/s are the angular velocities corresponding to the Earth's and standard days.

It can be seen that, during a tropical month, $v$ undergoes two semimonthly oscillations with maxima occurring at the maximum distance of the Moon from the celestial equator in both Northern and Southern hemispheres (i.e., at lunar solstices) and with minima occurring when the Moon intersects the equator (i.e., at lunar equinoxes).
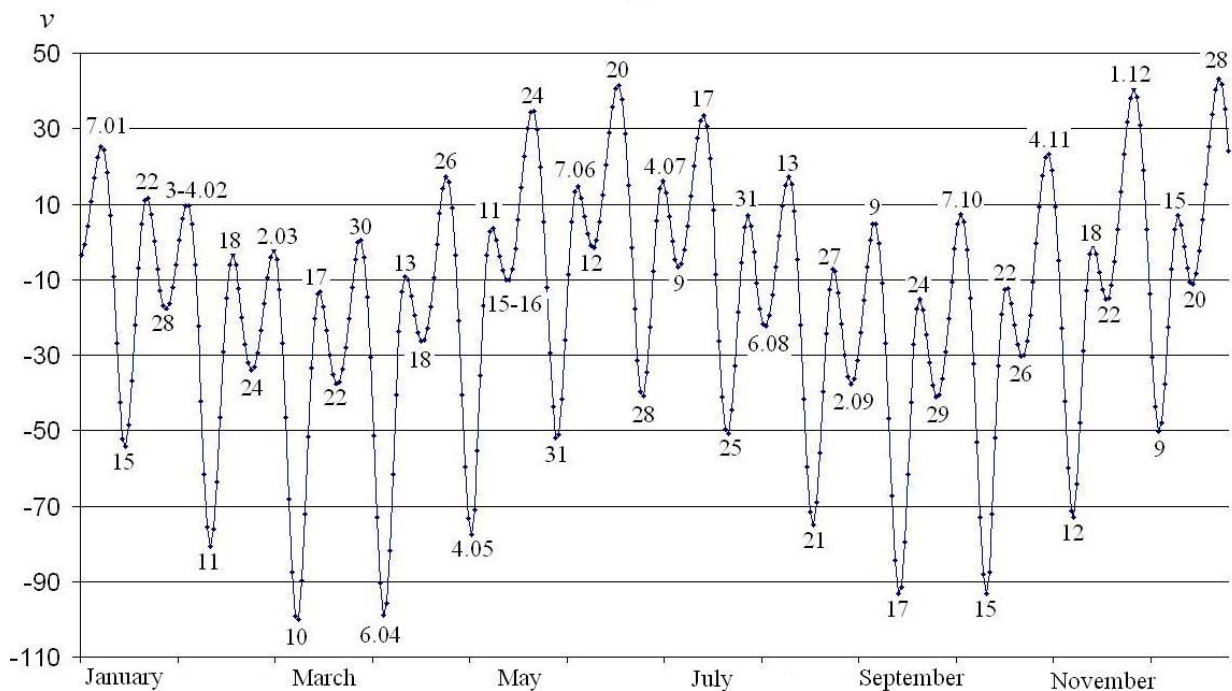


Figure 1. Tidal oscillations of the Earth's rotation velocity $v$ in 2016. The vertical axis represents the relative deviations of $v$ multiplied by $10^{10}$. Numerals indicate the dates when maxima and minima of $v$ occurred

The monitoring of tidal oscillations of $v$, the evolution of atmospheric synoptic processes, atmospheric circulation patterns, and time variations in hydrometeorological characteristics has

shown that most types of atmospheric synoptic processes vary **synchronously** with the tidal oscillations of the Earth's angular velocity (Sidorenkov, 2002, 2009). Using retrospective data, we verified how frequently the extrema (minima or maxima) of ν coincide in time with changes in elementary synoptic processes (ESP) in terms of the G.Ya. Vangengeim classification. A statistical analysis showed that 76% of the extrema of ν coincide in time (up to ±1 day) with ESP changes. In the other 24% of the cases, the extrema of ν are two and more days away from the nearest ESP change (Sidorenkov, 2002, 2009).

The long-time comparative monitoring of tidal oscillations of ν and variations in meteorological characteristics in Moscow, Vladivostok, Toronto, Buenos Aires and other sites clearly suggests that variations in meteorological characteristics agree in time with quasi-weekly extrema of ν (http://geoastro.ru ). Variations in weather elements at other sites of world have been monitored by S.P. Perov and L.V. Zotov. Their results also confirm that variations in meteorological characteristics are synchronized with oscillations of the Earth's angular velocity.

The tidal oscillations in the Earth's rotation velocity represent a perfect index for the features of the Earth's monthly rotation around the barycenter and time variations in the lunisolar tidal forces. They correlate with quasi-weekly and semimonthly variations in atmospheric processes and with local anomalies in the air temperature, pressure, cloudiness, and precipitation amounts depending on those variations.

Changes in weather patterns coincide with extrema of tidal oscillations of ν, which correspond to lunar solstices and lunar equinoxes. By analogy with three-month seasons of the year, which are associated with the Earth's rotation around the Sun, kind of quasi-weekly weather "seasons" can be identified in weather patterns.

Quantized weather patterns were first described by B.P. Mul'tanovskii (1933) 100 years ago. He called them natural synoptic periods (NSPs). The above observations suggest that Mul'tanovskii's NSPs are possibly caused by the monthly rotation of Earth and Moon around their barycenter. Weather is synchronized with the times of lunar equinoxes and solstices. In contrast to solar seasons, the lunar NSPs are not constant: they vary from 4 to 9 days with a mean of 6.8 days. These variations are caused by the frequency modulation of the tidal force oscillations due to the motion of the lunar perigee. Plots of tidal oscillations of ν provide a kind of NSP timetable, demonstrating that variations in NSP lengths are not random. Unfortunately, there still appear works in which the dynamics of NSPs is erroneously treated in terms of Brownian motion.

Note that synchronization does not determine the formation mechanisms of thermobaric structures due to the baroclinic instability of the atmosphere, but rather imposes evolution rhythms close to tidal force oscillations (more precisely, to rhythms in the Earth--Moon--Sun system) on atmospheric processes.

References

B.P. Mul'tanovskii, 1933: Basic Principles of Synoptic Method for Long-Term Weather Forecast. Moscow, TsUEGMS. [in Russian].

N.S. Sidorenkov, 2002: Physics of Instability in the Earth's Rotation. Moscow, Nauka. [in Russian].

N.S. Sidorenkov, 2009: The interaction between Earth's rotation and geophysical processes. Weinheim, WILEY-VCH Verlag GmbH & Co. KGaA.
http://www.geoastro.ru

N.S. Sidorenkov, T.S. Zhigailo, 2014: Atmospheric Effects of the Earth's Monthly Motion. In: WMO/WGNE Research Activities in atmospheric and oceanic modeling, WCRP Report No.11, pp.7-13--7-15.
http://www.wcrp-climate.org/WGNE/BlueBook/2014/individual-articles/07_Sidorenkov_Bluebook.pdf